

## Supplementary Information for

# Linear Coordination Polymers Based on Aluminum Phosphates: Synthesis, Crystal Structure and Morphology

M. Dębowski, K. Łokaj, A. Wolak, K. Żurawski, A. Plichta, J. Zachara, A. Ostrowski and Z. Florjańczyk

*Faculty of Chemistry, Warsaw University of Technology, Noakowskiego 3, 00-664 Warsaw, Poland.*

## Experimental

### Single-crystal structure analysis

Absorption effects were corrected using the multi-scan technique. The structure was solved in the centrosymmetric space group using direct methods in SHELXS-97 and refined using full-matrix least-squares against  $F^2$  in SHELXL-97.<sup>1</sup> However, the refinement converged at relatively high R values, with residual density in the difference Fourier map. Detailed inspection of the diffraction data revealed that the crystal was twinned by merohedry, with a 2-fold rotation about [001] or, correspondingly, the mirror plane perpendicular to [001] as a twin law. After introducing the twin law in the SHELXL-97 refinement, the value of the twin fraction was refined to 0.1326(4). One of the ethoxy groups [O(4)C(3)C(4)] was disordered over two sites. The disorder was modeled in terms of two sets of atoms with similarity restraints for chemically equivalent distances. The refined final occupancy factor for the major conformer was equal to 0.955(2). All non-hydrogen atoms were refined with anisotropic displacement parameters, excluding atoms in the minor component of the disordered region. Hydrogen atoms were introduced at calculated positions and constrained to ride on their parent atoms, with  $U_{\text{iso}}(\text{H}) = 1.2 \times U_{\text{eq}}(\text{C})$  or  $U_{\text{iso}}(\text{H}) = 1.5 \times U_{\text{eq}}(\text{C})$  in the case of methyl groups.

### Calculations of bond–valence vectors for aluminum and phosphorus centers

Bond valences were calculated using the most widely used equation describing the relationship between the bond length ( $d_{ij}$ ) between the  $i$ -th and  $j$ -th atoms and the valence of this bond ( $s_{ij}$ ):<sup>2</sup>

$$s_{ij} = \exp\left[\frac{r_{ij} - d_{ij}}{b}\right]$$

where  $r_{ij}$  and  $b$  are empirically determined constants for the given  $i$ – $j$  bond.  $r_{ij}$  is equal to the length of a conceptual bond of a unit valence, whereas the parameter  $b$  is generally treated as a ‘universal’ constant, often taken to be 0.37 Å.<sup>2,3</sup> The following parameters were used in the calculations:  $r_{\text{PO}} = 1.617$  Å ( $b = 0.37$  Å),<sup>2</sup> and  $r_{\text{AlO}} = 1.630$  Å ( $b = 0.37$  Å).<sup>4</sup>

According to the bond valence vector model,<sup>4</sup> the bond between the coordination center  $i$  and the more electronegative ligating atom  $j$  of  $s_{ij}$  valence can be represented by the bond-valence vector  $\mathbf{v}_{ij}$  directed from  $i$  to  $j$  with a length defined by the following equation:

$$|\mathbf{v}_{ij}| = s_{ij} \left(1 - \frac{s_{ij}}{Q_i}\right)$$

where  $Q_i$  is the charge in the core of the central  $i$ -th atom. The bond–valence vectors ( $\mathbf{v}_{\text{AlO}}$  and  $\mathbf{v}_{\text{PO}}$ ) and the resultant vectors ( $\mathbf{v}_{\text{Al}}$  and  $\mathbf{v}_{\text{P}}$ ) were calculated by setting the aluminum core charge  $Q_{\text{Al}} = 3$  and the phosphorus core charge  $Q_{\text{P}} = 5$ .

## Notes and references

- 1 G. M. Sheldrick, *Acta Crystallogr., Sect. A: Found. Crystallogr.*, 2008, **64**, 112.
- 2 I. D. Brown and D. Altermatt, *Acta Crystallogr., Sect. B: Struct. Sci.*, 1985, **41**, 244.
- 3 N. E. Brese and M. O’Keeffe, *Acta Crystallogr., Sect. B: Struct. Sci.*, 1991, **47**, 192.
- 4 J. Zachara, *Inorg. Chem.*, 2007, **46**, 9760.

**Table S1.** Symbols of symmetry operators for equivalent positions.

Symbol	Symmetry operators
<i>a</i>	-y, x-y, z
<i>b</i>	-x+y, -x, z
<i>c</i>	-x, -y, -z
<i>d</i>	-x, -y, 1-z
<i>e</i>	y, -x+y, -z
<i>f</i>	y, -x+y, 1-z
<i>g</i>	x-y, x, -z
<i>h</i>	x-y, x, 1-z
<i>i</i>	x, y, -1+z
<i>j</i>	x, y, 1+z
<i>k</i>	1-y, 1+x-y, -1+z
<i>l</i>	1-y, 1+x-y, z
<i>m</i>	1-y, 1+x-y, 1+z
<i>n</i>	-x+y, 1-x, -1+z
<i>o</i>	-x+y, 1-x, z
<i>p</i>	-x+y, 1-x, 1+z

**Table S2.** Selected bond lengths for DEPAI at -173(2) °C

Chain A		Chain B	
Bond	Distance/Å	Bond	Distance/Å
Al1-O1	1.8803(7)	Al11-O16 <sub><i>i</i></sub>	1.8768(7)
Al1-O1 <sub><i>a</i></sub>	1.8803(9)	Al11-O11	1.8808(8)
Al1-O1 <sub><i>b</i></sub>	1.8803(10)	Al11-O11 <sub><i>l</i></sub>	1.8808(10)
Al1-O1 <sub><i>c</i></sub>	1.8803(7)	Al11-O16 <sub><i>n</i></sub>	1.8768(10)
Al1-O1 <sub><i>e</i></sub>	1.8803(9)	Al11-O16 <sub><i>k</i></sub>	1.8768(10)
Al1-O1 <sub><i>g</i></sub>	1.8803(10)	Al11-O11 <sub><i>o</i></sub>	1.8808(11)
Al2-O2 <sub><i>a</i></sub>	1.8838(9)	Al12-O15	1.8917(8)
Al2-O2 <sub><i>f</i></sub>	1.8838(9)	Al12-O12 <sub><i>l</i></sub>	1.8898(10)
Al2-O2 <sub><i>b</i></sub>	1.8838(11)	Al12-O12	1.8898(9)
Al2-O2 <sub><i>d</i></sub>	1.8838(7)	Al12-O15 <sub><i>o</i></sub>	1.8917(12)
Al2-O2	1.8838(7)	Al12-O15 <sub><i>l</i></sub>	1.8917(10)
Al2-O2 <sub><i>h</i></sub>	1.8838(11)	Al12-O12 <sub><i>o</i></sub>	1.8898(9)
P1-O2	1.4946(7)	P11-O11	1.4969(8)
P1-O3	1.5806(8)	P11-O12	1.5018(7)
P1-O1	1.4944(8)	P11-O13	1.5753(8)
P1-O4	1.5843(11)	P11-O14	1.5802(9)
P1-*O4B	1.565(19)	P12-O15	1.5027(7)
O3-C1	1.4505(13)	P12-O16	1.4965(7)
O4-C3	1.4538(14)	P12-O17	1.5732(9)
*O4B-*C3B	1.44(3)	P12-O18	1.5805(9)
C1-C2	1.5050(19)	O17-C15	1.4486(13)
C3-C4	1.502(2)	O18-C17	1.4538(15)
*C3B-*C4B	1.51(4)	O13-C11	1.4488(14)
		O14-C13	1.4547(13)
		C11-C12	1.5055(15)
		C13-C14	1.5071(19)
		C15-C16	1.501(2)
		C17-C18	1.5039(18)

*a-p* – symbols of translation symmetry for equivalent positions defined in Table S2.

**Table S3.** Selected bond angles for DEPAI at -173(2) °C

Chain A		Chain B	
Bond	Angle/°	Bond	Angle/°
O3-P1-*O4B	89.5(7)	O11-P11-O12	117.01(5)
O1-P1-O2	118.82(4)	O11-P11-O13	105.47(4)
O1-P1-O3	104.14(5)	O11-P11-O14	111.23(4)
O1-P1-O4	111.37(5)	O12-P11-O13	112.08(4)
O1-P1-*O4B	113.8(7)	O12-P11-O14	108.56(4)
O2-P1-O3	111.52(4)	O13-P11-O14	101.37(5)
O2-P1-O4	103.98(5)	O15-P12-O16	117.23(4)
O2-P1-*O4B	114.4(7)	O15-P12-O17	112.04(4)
O3-P1-O4	106.56(5)	O15-P12-O18	108.39(5)
		O16-P12-O17	105.18(5)
		O16-P12-O18	111.11(4)
		O17-P12-O18	101.82(4)
O1-Al1-O1_a	91.16(4)	O11-Al11-O16_j	88.98(3)
O1-Al1-O1_b	91.16(3)	O11_l-Al11-O16_k	88.98(4)
O1-Al1-O1_c	180.00	O16_k-Al11-O16_n	91.09(5)
O1-Al1-O1_e	88.84(4)	O11_o-Al11-O16_k	179.81(4)
O1-Al1-O1_g	88.84(3)	O11_l-Al11-O16_n	89.09(4)
O1_a-Al1-O1_b	91.16(4)	O11_l-Al11-O11_o	90.85(4)
O1_a-Al1-O1_c	88.84(4)	O11_o-Al11-O16_n	88.98(4)
O1_a-Al1-O1_e	180.00	O11_o-Al11-O16_j	89.09(3)
O1_e-Al1-O1_g	91.16(4)	O11-Al11-O11_l	90.85(4)
O1_a-Al1-O1_g	88.84(4)	O11-Al11-O16_n	179.81(4)
O1_b-Al1-O1_c	88.84(3)	O11-Al11-O11_o	90.85(4)
O1_b-Al1-O1_e	88.84(4)	O16_j-Al11-O16_k	91.09(4)
O1_b-Al1-O1_g	180.00	O11_l-Al11-O16_j	179.81(4)
O1_c-Al1-O1_e	91.16(4)	O16_j-Al11-O16_n	91.09(4)
O1_c-Al1-O1_g	91.16(3)	O11-Al11-O16_k	89.09(4)
O2-Al2-O2_a	91.35(4)	O12-Al12-O15_l	89.06(4)
O2-Al2-O2_b	91.35(4)	O12-Al12-O12_o	90.99(4)
O2-Al2-O2_d	180.00	O12-Al12-O15_o	180.00
O2-Al2-O2_f	88.65(4)	O12_l-Al12-O15	180.00
O2-Al2-O2_h	88.65(4)	O15-Al12-O15_l	91.00(4)
O2_a-Al2-O2_b	91.35(4)	O12_o-Al12-O15	89.06(3)
O2_a-Al2-O2_d	88.65(4)	O12-Al12-O15	88.96(3)
O2_a-Al2-O2_f	180.00	O12-Al12-O12_l	90.99(4)
O2_f-Al2-O2_h	91.35(4)	O12_o-Al12-O15_o	88.96(4)
O2_b-Al2-O2_f	88.65(4)	O15-Al12-O15_o	91.00(4)
O2_a-Al2-O2_h	88.65(4)	O12_l-Al12-O15_l	88.96(4)
O2_b-Al2-O2_d	88.65(4)	O12_l-Al12-O12_o	90.99(4)
O2_d-Al2-O2_h	91.35(4)	O12_l-Al12-O15_o	89.06(4)
O2_b-Al2-O2_h	180.00	O12_o-Al12-O15_l	180.00
O2_d-Al2-O2_f	91.35(4)	O15_l-Al12-O15_o	91.00(4)
P1-O1-Al1	139.74(5)	P11-O11-Al11	141.88(5)
P1-O2-Al2	138.88(6)	P11-O12-Al12	138.24(5)
		P12-O15-Al12	138.05(6)
		P12-O16-Al11_j	141.82(6)
P1-O3-C1	118.83(8)	P11-O14-C13	119.80(8)
P1-O4-C3	118.62(9)	P11-O13-C11	118.56(6)
P1-*O4B-*C3B	113.5(13)	P12-O17-C15	119.17(8)
		P12-O18-C17	119.60(6)
O3-C1-C2	107.69(10)	O13-C11-C12	108.00(9)
O4-C3-C4	107.65(11)	O14-C13-C14	107.73(9)
*O4B-*C3B-*C4B	108(2)	O17-C15-C16	108.15(10)
		O18-C17-C18	108.05(9)

*a-p* – symbols of translation symmetry for equivalent positions defined in Table S2.

**Table S4.** Selected torsion angles for DEPAL at  $-173(2)$  °C

Bond	Angle/°	Bond	Angle/°
O2–P1–O1–Al1	44.21(10)	O1–P1–O2–Al2	45.99(9)
O3–P1–O1–Al1	168.99(7)	O3–P1–O2–Al2	-75.12(8)
O4–P1–O1–Al1	-76.54(8)	O4–P1–O2–Al2	170.43(7)
O12–P11–O11–Al11	40.70(10)	O15–P12–O16–Al11 <sub>j</sub>	-40.10(10)
O13–P11–O11–Al11	166.08(8)	O17–P12–O16–Al11 <sub>j</sub>	-165.32(8)
O14–P11–O11–Al11	-84.84(9)	O18–P12–O16–Al11 <sub>j</sub>	85.28(8)
O11–P11–O12–Al12	51.19(8)	O16–P12–O15–Al12	-51.34(9)
O13–P11–O12–Al12	-70.81(8)	O17–P12–O15–Al12	70.39(8)
O14–P11–O12–Al12	178.06(6)	O18–P12–O15–Al12	-178.06(6)
O1–P1–O3–C1	-176.60(7)	O1–P1–O4–C3	-43.70(9)
O2–P1–O3–C1	-47.27(9)	O2–P1–O4–C3	-172.82(8)
O4–P1–O3–C1	65.57(8)	O3–P1–O4–C3	69.26(8)
O11–P11–O13–C11	177.58(8)	O11–P11–O14–C13	66.95(8)
O12–P11–O13–C11	-54.04(9)	O12–P11–O14–C13	-63.17(8)
O14–P11–O13–C11	61.55(9)	O13–P11–O14–C13	178.67(7)
O15–P12–O17–C15	51.80(9)	O15–P12–O18–C17	63.07(8)
O16–P12–O17–C15	-179.80(7)	O16–P12–O18–C17	-67.11(8)
O18–P12–O17–C15	-63.82(8)	O17–P12–O18–C17	-178.68(7)
O1 <sub>b</sub> –Al1–O1–P1	-92.48(8)	O1 <sub>σ</sub> –Al1–O1–P1	-1.29(8)
O1 <sub>e</sub> –Al1–O1–P1	178.71(8)	O1 <sub>g</sub> –Al1–O1–P1	87.52(8)
O2 <sub>f</sub> –Al2–O2–P1	86.88(7)	O2 <sub>b</sub> –Al2–O2–P1	-1.74(7)
O2 <sub>α</sub> –Al2–O2–P1	-93.12(7)	O2 <sub>h</sub> –Al2–O2–P1	178.26(7)
O16 <sub>j</sub> –Al11–O11–P11	179.35(9)	O12 <sub>j</sub> –Al12–O12–P11	-95.84(7)
O16 <sub>k</sub> –Al11–O11–P11	88.24(9)	O15 <sub>j</sub> –Al12–O12–P11	175.22(7)
O11 <sub>l</sub> –Al11–O11–P11	-0.72(9)	O12 <sub>o</sub> –Al12–O12–P11	-4.84(7)
O11 <sub>o</sub> –Al11–O11–P11	-91.58(9)	O15–Al12–O12–P11	84.20(7)
O12–Al12–O15–P12	-175.21(7)	O12 <sub>o</sub> –Al12–O15–P12	-84.20(8)
O15 <sub>l</sub> –Al12–O15–P12	95.76(7)	O15 <sub>o</sub> –Al12–O15–P12	4.74(7)
P1–O3–C1–C2	172.00(7)	P1–O4–C3–C4	175.28(9)
P11–O13–C11–C12	170.90(8)	P11–O14–C13–C14	-149.13(8)
P12–O17–C15–C16	-176.67(8)	P12–O18–C17–C18	159.42(8)

*a-p* – symbols of translation symmetry for equivalent positions defined in Table S2.

**Table S5.** Intermolecular hydrogen bonding C–H...O for DEPAL at  $-173(2)$  °C

D–H...A system	D–H distance/Å	H...A distance/Å	D...A distance/Å	D–H...A angle/°
C1–H1A...O2 <sub>f</sub>	0.99	2.49	3.3255(14)	142
C3–H3A...O1 <sub>g</sub>	0.99	2.41	3.2909(13)	148
C13–H13B...O11 <sub>l</sub>	0.99	2.53	3.3993(17)	147
C13–H13B...O16 <sub>k</sub>	0.99	2.53	3.3128(14)	136
C15–H15B...O12 <sub>o</sub>	0.99	2.51	3.3403(13)	141
C17–H17A...O11 <sub>j</sub>	0.99	2.45	3.3140(13)	145

*D, A* – hydrogen donor and acceptor, respectively; *a-p* – symbols of translation symmetry for equivalent positions defined in Table S2.

**Table S6.** X-ray powder diffraction data for DEPAL measured at 25 °C.

Index	2 $\theta$ /°	d Value/Å	Rel. Intensity	Index	2 $\theta$ /°	d Value/Å	Rel. Intensity
1	8.466	10.436	100.0%	16	27.724	3.215	0.7%
2	13.839	6.394	0.3%	17	29.022	3.074	1.1%
3	14.653	6.040	0.2%	18	29.851	2.991	0.3%
4	16.218	5.461	1.1%	19	31.437	2.843	0.3%
5	16.897	5.243	0.3%	20	32.617	2.743	0.7%
6	17.592	5.037	0.1%	21	33.713	2.656	0.3%
7	19.696	4.504	1.1%	22	35.829	2.504	0.2%
8	20.184	4.396	4.2%	23	36.830	2.438	0.1%
9	21.386	4.151	0.2%	24	39.823	2.262	0.1%
10	21.895	4.056	1.7%	25	43.617	2.073	0.0%
11	22.377	3.970	4.8%	26	45.473	1.993	0.2%
12	23.501	3.782	5.6%	27	47.996	1.894	0.2%
13	24.504	3.630	0.5%	28	51.968	1.758	0.2%
14	25.982	3.427	0.5%	29	53.503	1.711	0.1%
15	26.383	3.375	1.7%	30	54.278	1.689	0.1%

**Table S7.** X-ray powder diffraction data for DEPAL calculated based on the data collected by single-crystal X-ray analysis at -173(2) °C.

Index	2 $\theta$ /°	d Value/Å	Rel. Intensity	Index	2 $\theta$ /°	d Value/Å	Rel. Intensity
1	8.645	10.220	100.0%	44	41.905	2.154	1.3%
2	13.102	6.752	0.7%	45	42.997	2.102	0.2%
3	14.025	6.310	0.7%	46	43.326	2.087	0.1%
4	16.502	5.368	2.9%	47	43.479	2.080	0.1%
5	17.965	4.934	3.9%	48	44.278	2.044	0.2%
6	19.978	4.441	2.9%	49	44.771	2.023	0.3%
7	20.363	4.358	4.5%	50	44.879	2.018	0.3%
8	20.584	4.311	4.9%	51	45.182	2.005	0.2%
9	22.379	3.969	4.8%	52	45.477	1.993	0.1%
10	23.017	3.861	5.5%	53	46.102	1.967	0.7%
11	23.822	3.732	5.9%	54	46.584	1.948	1.3%
12	23.977	3.708	1.0%	55	47.021	1.931	0.9%
13	25.078	3.548	4.8%	56	47.879	1.898	0.1%
14	26.864	3.316	9.7%	57	48.177	1.887	0.1%
15	27.042	3.295	1.3%	58	48.339	1.881	0.7%
16	28.022	3.182	0.6%	59	48.763	1.866	0.2%
17	28.280	3.153	2.6%	60	49.202	1.850	0.4%
18	28.424	3.137	1.6%	61	49.640	1.835	0.5%
19	29.613	3.014	5.3%	62	50.077	1.820	0.3%
20	29.789	2.997	2.9%	63	50.439	1.808	0.1%
21	30.264	2.951	0.4%	64	50.788	1.796	0.0%
22	31.905	2.803	0.8%	65	51.018	1.789	0.2%
23	32.308	2.769	0.1%	66	51.303	1.779	0.5%
24	32.720	2.735	0.1%	67	51.844	1.762	0.1%
25	33.125	2.702	1.0%	68	52.103	1.754	0.1%
26	33.361	2.684	0.7%	69	52.657	1.737	0.0%
27	34.517	2.596	1.6%	70	52.983	1.727	0.1%
28	34.679	2.585	0.9%	71	53.209	1.720	0.1%
29	35.042	2.559	0.5%	72	53.398	1.714	0.3%
30	36.160	2.482	0.4%	73	53.796	1.703	0.6%
31	36.784	2.441	1.5%	74	54.581	1.680	1.0%
32	36.902	2.434	0.6%	75	55.000	1.668	0.5%
33	37.241	2.412	0.4%	76	55.363	1.658	0.8%
34	37.454	2.399	0.1%	77	55.804	1.646	0.1%
35	37.965	2.368	0.6%	78	56.184	1.636	0.2%
36	38.362	2.344	0.1%	79	56.360	1.631	0.2%
37	38.885	2.314	0.5%	80	56.559	1.626	0.1%
38	39.355	2.288	0.6%	81	57.200	1.609	0.1%
39	39.703	2.268	0.4%	82	57.716	1.596	0.7%
40	40.383	2.232	0.4%	83	58.138	1.585	0.1%
41	40.924	2.203	0.8%	84	58.462	1.577	0.4%
42	41.363	2.181	0.4%	85	58.964	1.565	0.3%
43	41.680	2.165	0.2%	86	59.240	1.558	0.4%

**Table S8.** X-ray powder diffraction data for DMPAl measured at 25 °C.

Index	2 $\theta$ /°	d Value/Å	Rel. Intensity
1	9.679	9.1307	100.0%
2	9.770	9.0458	95.0%
3	10.781	8.1995	12.9%
4	13.786	6.4183	0.4%
5	16.633	5.3256	0.9%
6	18.850	4.7039	5.6%
7	19.403	4.5710	0.3%
8	19.627	4.5192	4.4%
9	20.536	4.3213	16.4%
10	21.218	4.1840	0.6%
11	21.890	4.0570	0.3%
12	22.400	3.9657	0.4%
13	23.828	3.7313	0.6%
14	24.900	3.5730	1.0%
15	25.021	3.5559	2.2%
16	25.474	3.4938	1.8%
17	26.022	3.4213	1.5%
18	26.707	3.3351	4.1%
19	27.672	3.2210	4.2%
20	28.308	3.1500	0.4%
21	28.747	3.1029	3.5%
22	29.229	3.0528	0.4%
23	29.918	2.9841	1.1%
24	30.302	2.9472	1.0%
25	31.788	2.8127	0.5%
26	33.146	2.7005	1.0%
27	33.556	2.6684	0.4%
28	33.931	2.6398	0.5%
29	35.381	2.5349	0.6%
30	37.807	2.3776	1.5%
31	38.309	2.3476	0.4%
32	38.463	2.3385	0.6%
33	39.107	2.3015	0.3%
34	41.690	2.1647	0.3%
35	44.086	2.0524	0.3%
36	45.676	1.9846	0.3%
37	49.564	1.8376	0.4%
38	52.275	1.7486	0.4%
39	54.915	1.6706	0.2%
40	56.986	1.6147	0.2%
41	59.647	1.5488	0.2%

**Table S9.** X-ray powder diffraction data for DnPPAl measured at 25 °C.

Index	2 $\theta$ /°	d Value/Å	Rel. Intensity
1	7.516	11.7524	100.0%
2	12.987	6.8114	1.6%
3	14.968	5.9138	0.1%
4	16.210	5.4634	0.2%
5	17.872	4.9590	0.3%
6	19.873	4.4640	6.6%
7	21.232	4.1812	0.1%
8	22.132	4.0132	2.3%
9	22.543	3.9408	1.0%
10	24.576	3.6193	0.9%
11	26.058	3.4168	0.1%
12	27.222	3.2733	0.1%
13	27.864	3.1993	0.5%
14	28.891	3.0878	0.6%
15	31.777	2.8137	0.1%
16	34.447	2.6014	0.3%
17	36.129	2.4841	0.2%
18	40.315	2.2353	0.1%
19	41.547	2.1718	0.1%
20	42.524	2.1241	0.1%
21	47.979	1.8946	0.2%
22	50.545	1.8043	0.1%
23	54.175	1.6916	0.1%

**Table S10.** X-ray powder diffraction data for DiPPAI measured at 25 °C.

Index	2 $\theta$ /°	d Value/Å	Rel. Intensity
1	7.761	11.3819	100.0%
2	15.474	5.7215	0.3%
3	16.412	5.3968	1.7%
4	18.696	4.7423	0.6%
5	19.014	4.6636	0.6%
6	19.490	4.5508	0.5%
7	20.483	4.3323	5.1%
8	22.555	3.9388	2.8%
9	23.259	3.8212	0.5%
10	24.638	3.6103	0.5%
11	24.913	3.5711	0.4%
12	26.751	3.3298	0.3%
13	27.329	3.2607	0.2%
14	28.072	3.1760	1.8%
15	28.599	3.1186	2.5%
16	29.649	3.0105	0.8%
17	30.528	2.9259	0.3%
18	31.052	2.8777	0.2%
19	34.030	2.6324	0.2%
20	35.411	2.5328	0.8%
21	40.475	2.2268	0.1%
22	41.617	2.1683	0.2%
23	41.987	2.1500	0.3%
24	43.908	2.0604	0.2%
25	47.529	1.9115	0.2%

**Table S11.** X-ray powder diffraction data for DBPAI<sup>a</sup> measured at 25 °C.

Index	2 $\theta$ /°	d Value/Å	Rel. Intensity
1	6.635	13.311	100.0%
2	11.608	7.617	2.1%
3	15.198	5.825	0.5%
4	17.837	4.968	4.1%
5	19.478	4.554	5.6%
6	20.307	4.369	8.1%
7	21.870	4.061	3.8%
8	22.462	3.955	4.3%
9	25.460	3.496	0.7%
10	26.296	3.386	1.8%
11	52.826	1.732	0.4%
12	58.443	1.578	0.3%

<sup>a</sup> sample prepared from TEA and DBP (DOP-TEA synthetic route).

**Table S12.** X-ray powder diffraction data for BEHPAI<sup>a</sup> measured at 25 °C.

Index	2 $\theta$ /°	d Value/Å	Rel. Intensity
1	5.353	16.496	100.0%
2	9.276	9.526	4.3%
3	14.243	6.213	14.9%
4	16.208	5.464	0.7%
5	18.238	4.860	1.8%
6	18.842	4.706	1.4%
7	19.529	4.542	19.1%
8	19.759	4.489	15.8%
9	21.223	4.183	11.6%
10	21.664	4.099	4.6%
11	23.610	3.765	1.5%
12	24.487	3.632	1.8%
13	24.847	3.581	2.2%
14	25.202	3.531	1.7%
15	28.468	3.133	0.7%
16	31.150	2.869	0.3%

<sup>a</sup> sample prepared from Allact and sodium salt of BEHP (DOPNa synthetic route).

**Table S13.** X-ray powder diffraction data for DPhPAI<sup>a</sup> measured at 25 °C.

Index	2 $\theta$ /°	d Value/Å	Rel. Intensity
1	6.730	13.1238	100.0%
2	11.626	7.6051	0.3%
3	13.488	6.5591	0.4%
4	16.698	5.3048	0.6%
5	17.910	4.9485	3.4%
6	19.572	4.5320	6.8%
7	20.401	4.3496	7.7%
8	23.865	3.7255	0.4%
9	24.899	3.5730	0.3%
10	26.630	3.3446	0.5%
11	28.258	3.1555	0.4%
12	30.884	2.8930	0.4%

<sup>a</sup> sample prepared from Allact and sodium salt of DPhP (DOPNa synthetic route).

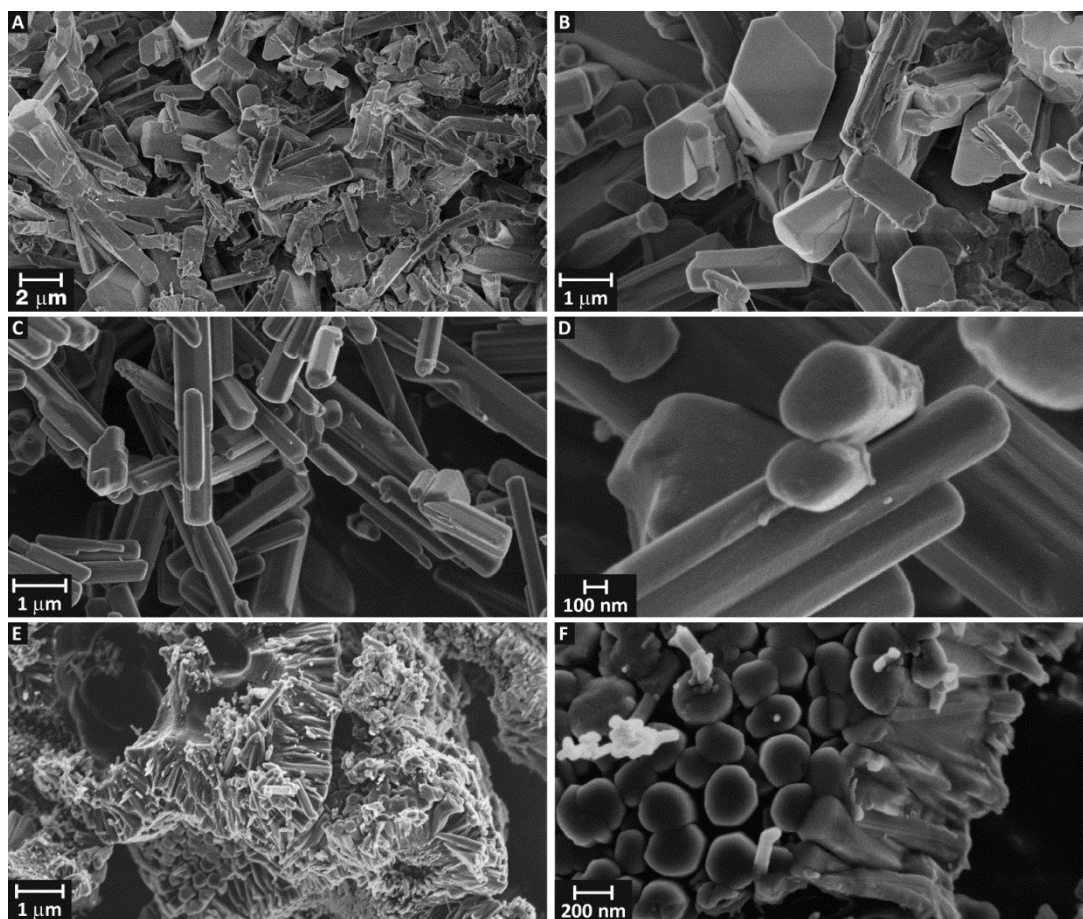


**Figure S1.** SEM images of DPhPAI synthesized from Allact and DPhP (DOP synthetic route, *Method M3*) (A–D), or its sodium salt (DOPNa synthetic route) (E–F). DPhPAI sample obtained after 1 h (A, B) or 24 h (C, D) of heating at 130 °C.

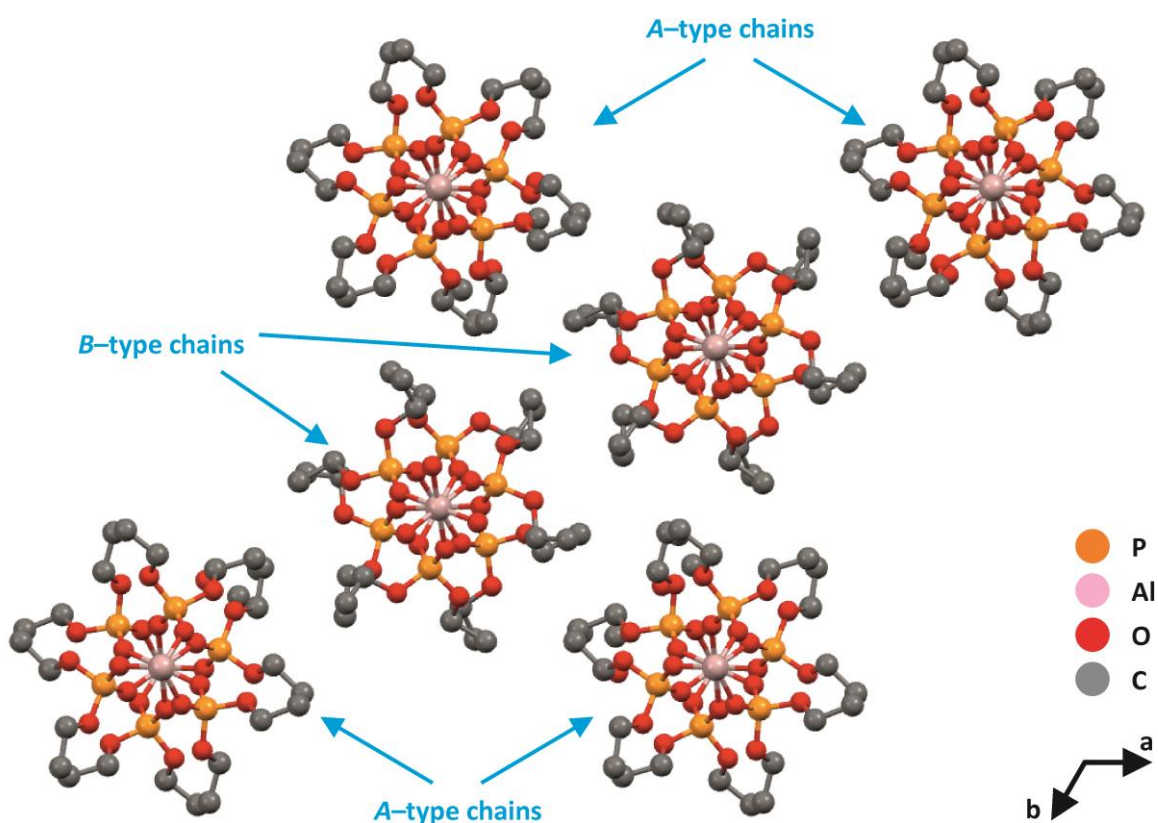


**Figure S2.** Crystallographic unit cell of DEPAI. The view is down the  $c$ -axis.

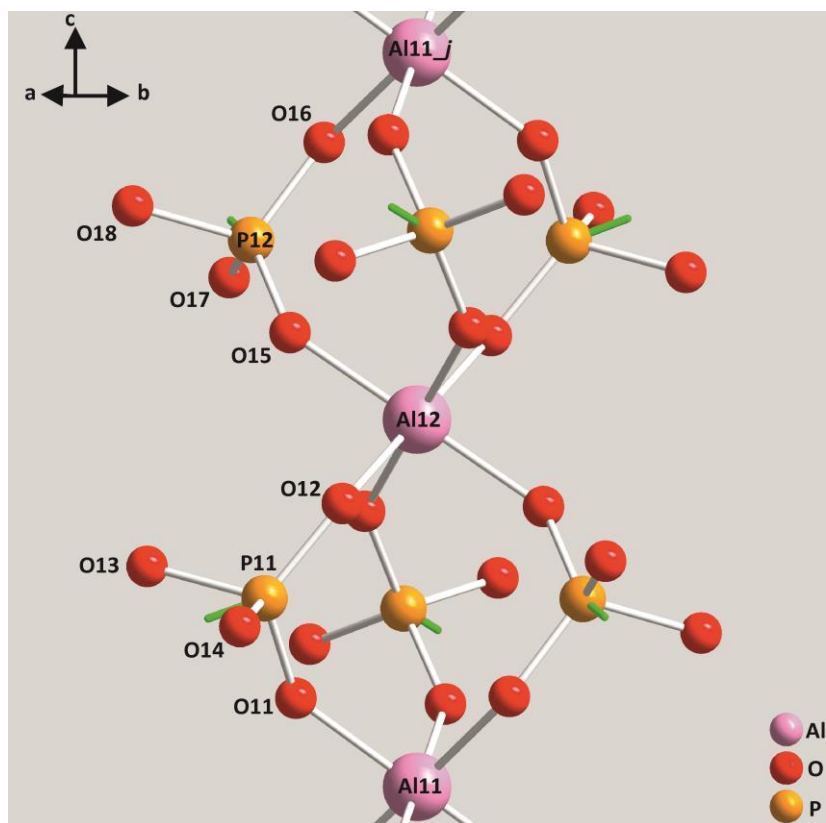


**Figure S3.** Resultant bond–valence vector at phosphorus center (in green) for *B*-type DEPAI chain. For the graphical presentation, it was assumed that 1 v.u. is equal to 10 Å, and the carbon and hydrogen atoms were omitted.

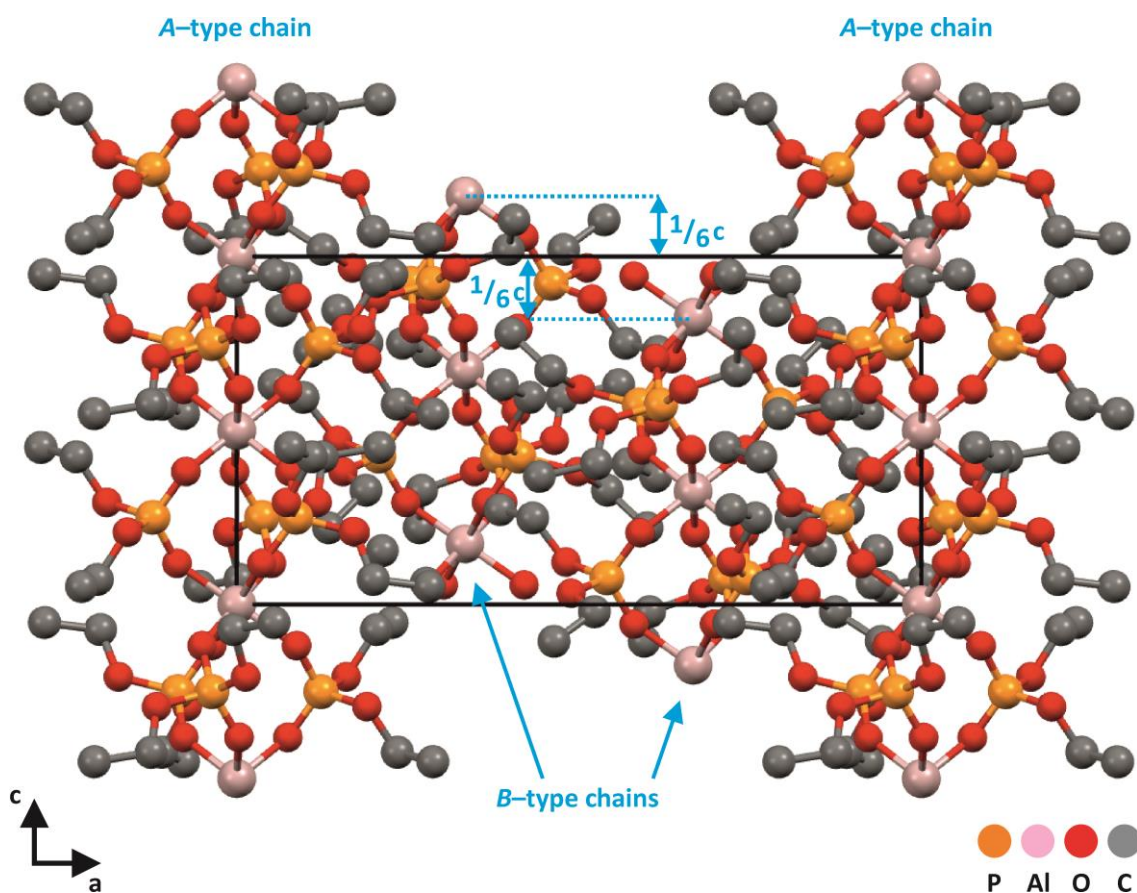


**Figure S4.** Crystal structure of DEPAI. The view is down the crystallographic *b*-axis. The edges of the DEPAI unit cell are indicated by black solid lines.

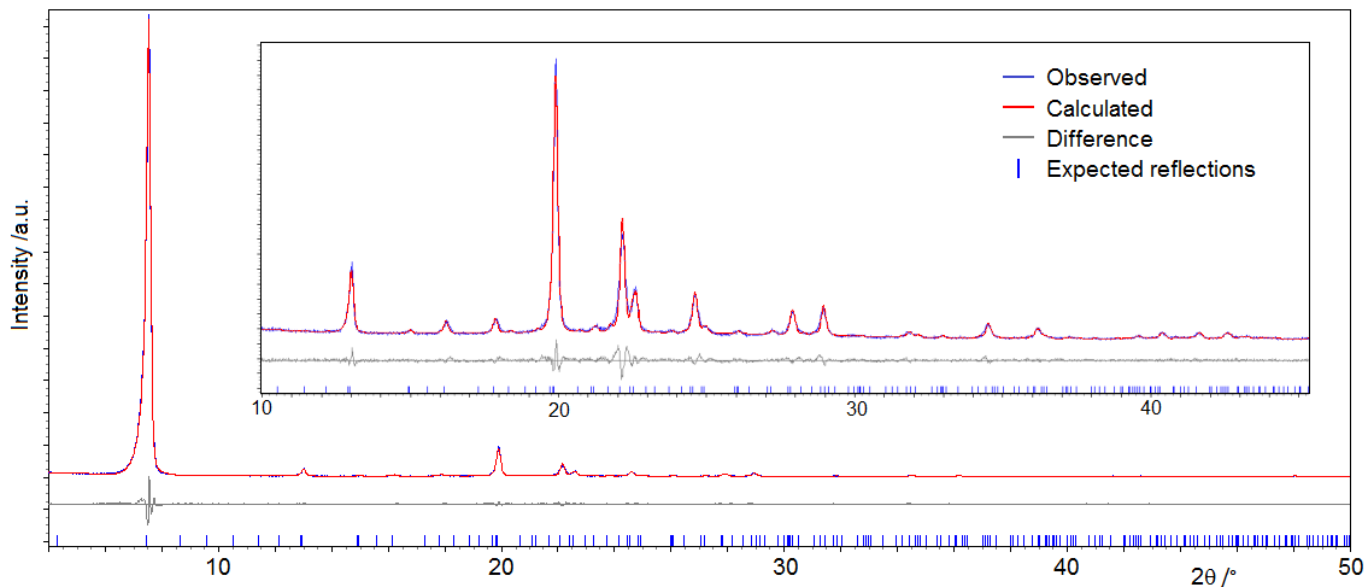


**Figure S5.** Pawley fit of DnPPAI. Cell refined to  $a = 23.6600(11)$  Å,  $c = 9.2316(10)$  Å (space group  $P\bar{3}$ ),  $R_{wp} = 7.44\%$ .

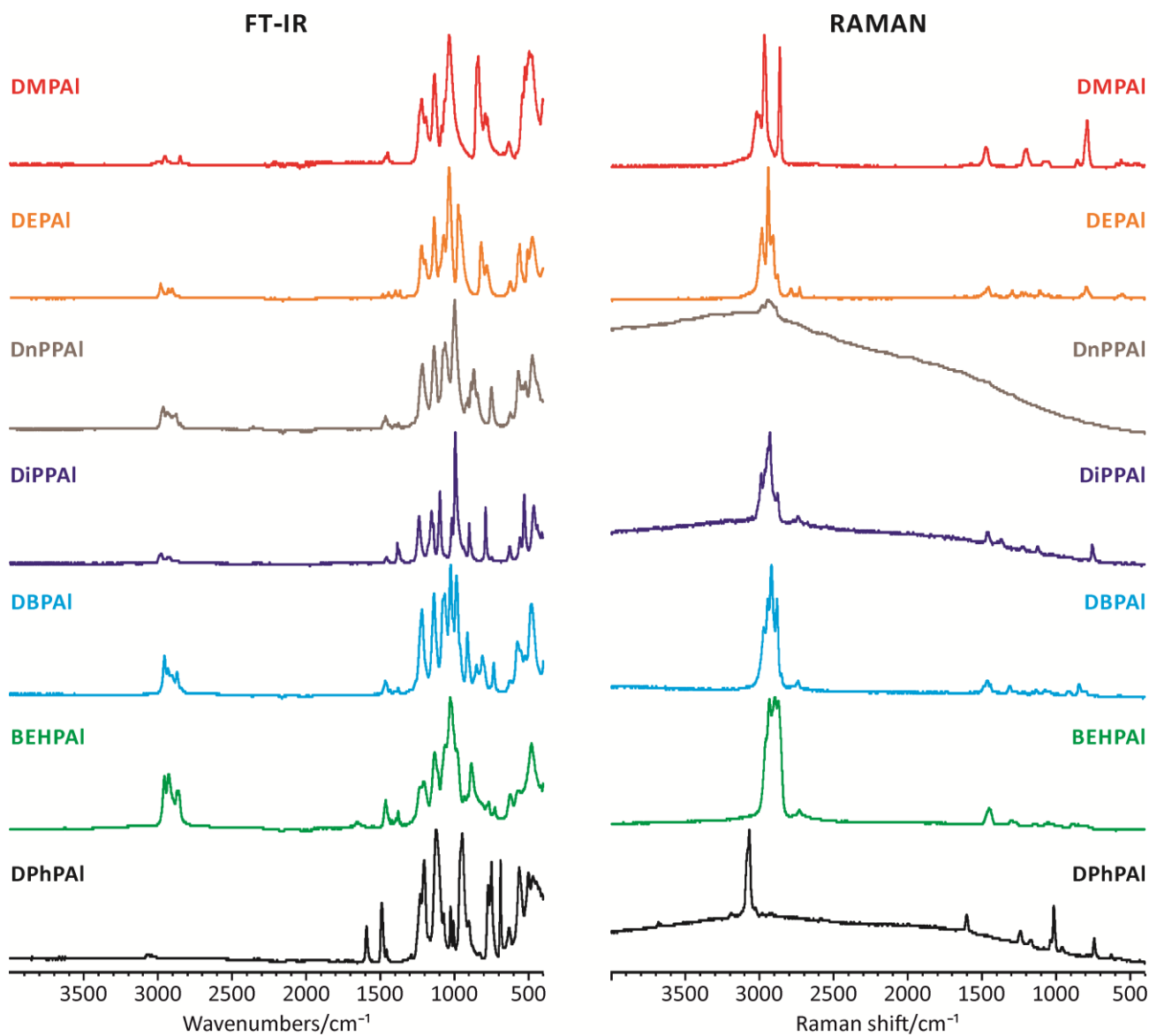


**Figure S6.** FT-IR (*left*) and Raman (*right*) spectra of DOPAI samples. The butyl, 2-ethylhexyl or phenyl derivatives were synthesized from: TEA and DOP (DBPAI), or AlLact and DOPNa (BEHPAI and DPhPAI).

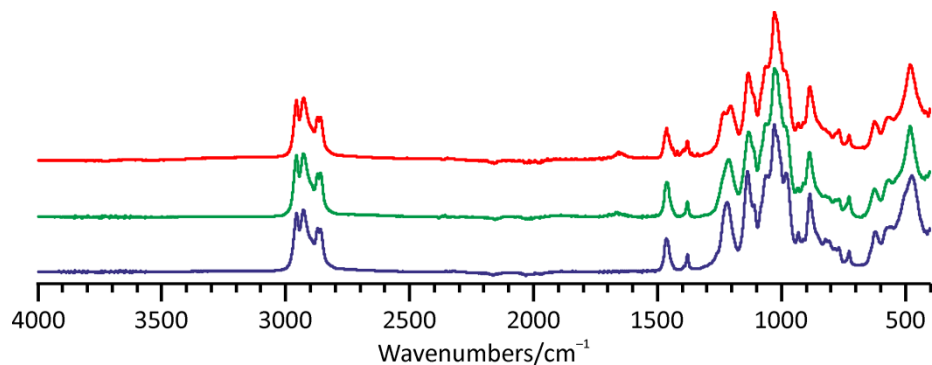


**Figure S7.** FT-IR spectra of BEHPAL samples synthesized by different methods: DOPNa synthetic route (red), DOP synthetic route, *Method M2* (green) and DOP-TEA synthetic route (dark blue).

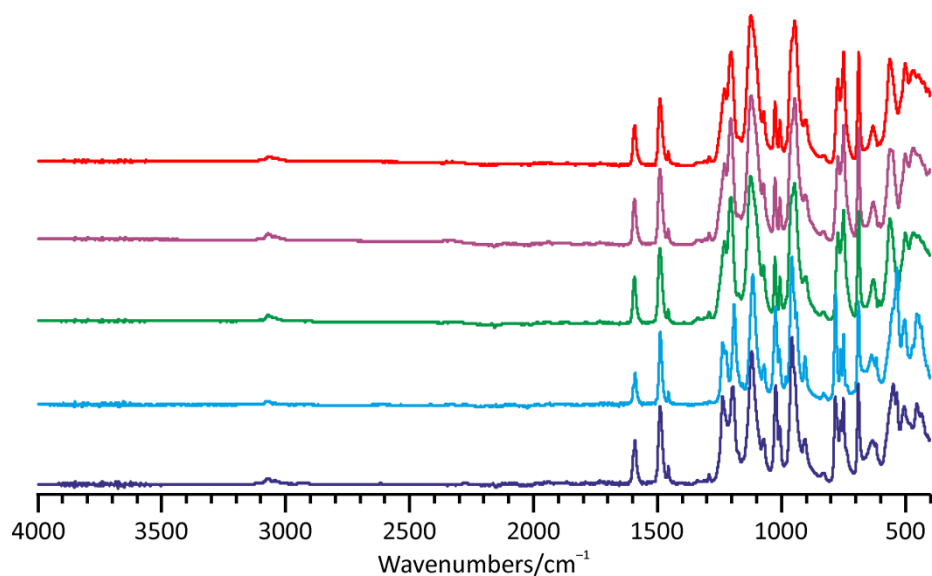


**Figure S8.** FT-IR spectra of DPhPAL samples synthesized by different methods: DOPNa synthetic route (red); DOP synthetic route, *Method M3* after 24 h (purple) or 1 h of heating (green); TOP synthetic route, *Method M3* (blue) and *Method M2* (dark blue).

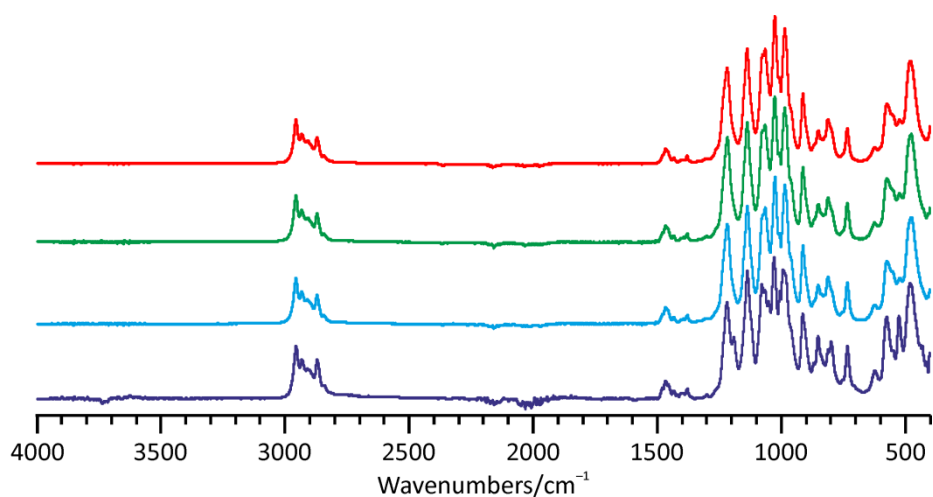


**Figure S9.** FT-IR spectra of DBPAL samples synthesized by different methods: DOP-TEA synthetic route (red); DOPNa synthetic route (green); DOP synthetic route, *Method M1* (blue); TOP synthetic route, *Method M2* (dark blue).

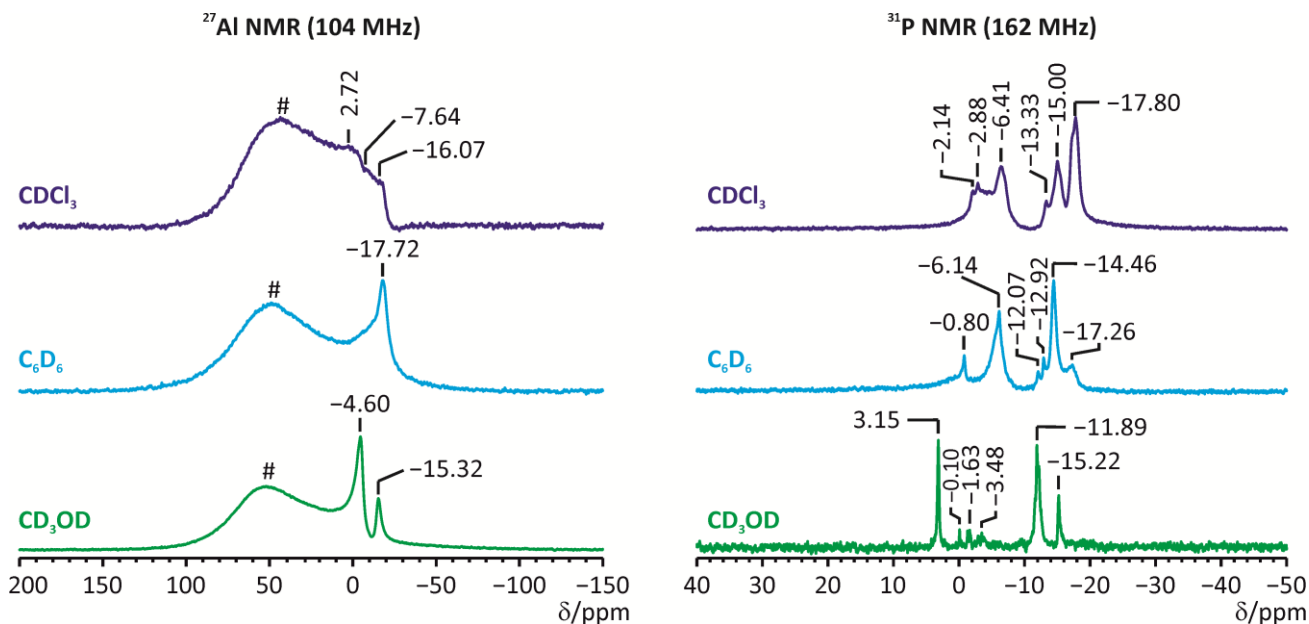


**Figure S10.**  $^{27}\text{Al}$  (left) and  $^{31}\text{P}$  (right) NMR spectra of BEHPAI (synthesized according to DOP synthetic route, Method M2) dispersed in  $\text{CDCl}_3$  (dark blue),  $\text{C}_6\text{D}_6$  (blue), or  $\text{CD}_3\text{OD}$  (green). The spectra were recorded at ambient temperature. The # symbols indicate artificial NMR probe signals. All chemical shifts are reported relative to  $[\text{Al}(\text{H}_2\text{O})_6]^{3+}$  ( $^{27}\text{Al}$ ) or 85%  $\text{H}_3\text{PO}_4$  ( $^{31}\text{P}$ ) external standards.

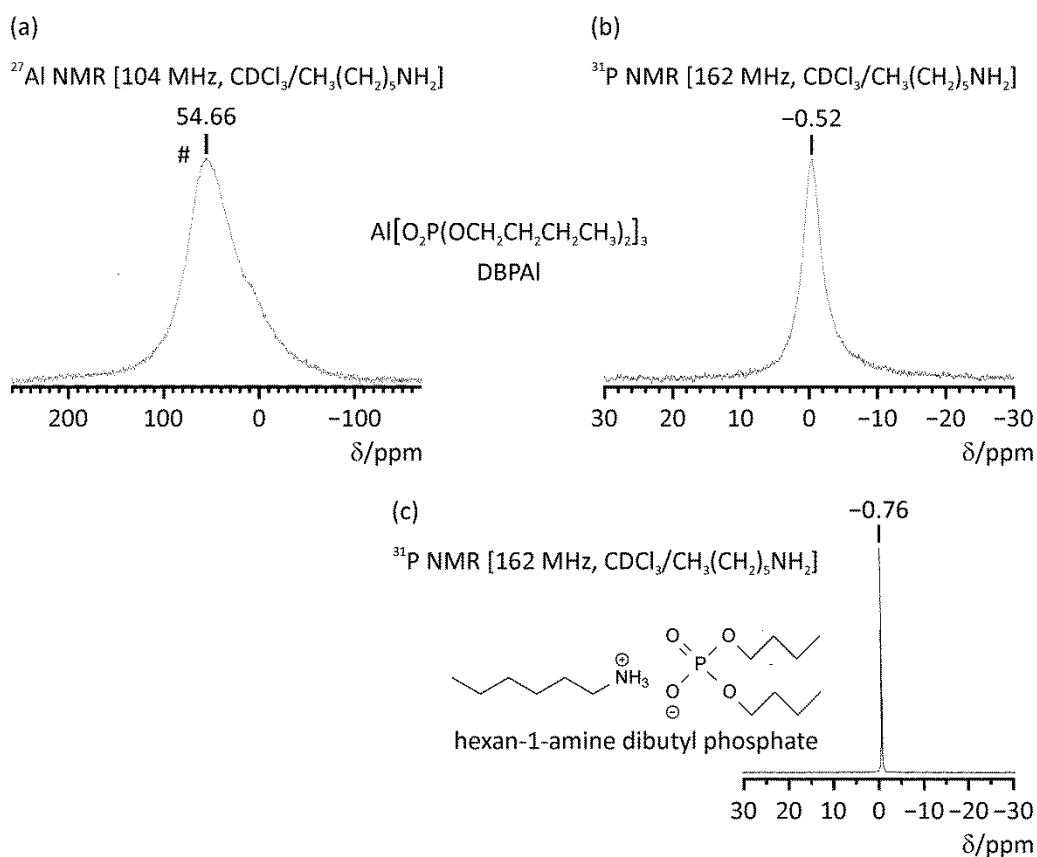


**Figure S11.**  $^{27}\text{Al}$  (a),  $^{31}\text{P}$  (b) NMR spectra of DBPAI, and  $^{31}\text{P}$  (c) NMR spectrum of hexan-1-amine dibutyl phosphate. All samples were dissolved in a 1:2 (v/v) mixture of  $\text{CDCl}_3$  and hexan-1-amine. The spectra were recorded at ambient temperature. The # symbol indicates an artificial NMR probe signal. All chemical shifts are reported relative to  $[\text{Al}(\text{H}_2\text{O})_6]^{3+}$  ( $^{27}\text{Al}$ ) or 85%  $\text{H}_3\text{PO}_4$  ( $^{31}\text{P}$ ) external standards.

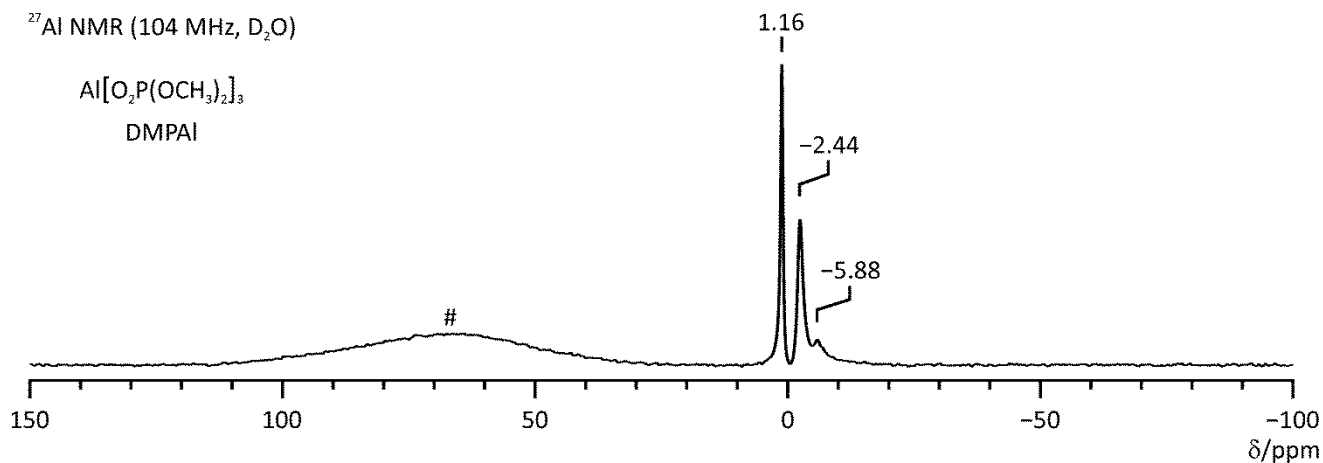


**Figure S12.** <sup>27</sup>Al NMR spectrum of DMPAI dissolved in D<sub>2</sub>O. The spectrum was recorded at ambient temperature. The # symbol indicates an artificial NMR probe signal. The chemical shifts are reported relative to [Al(H<sub>2</sub>O)<sub>6</sub>]<sup>3+</sup> external standard.

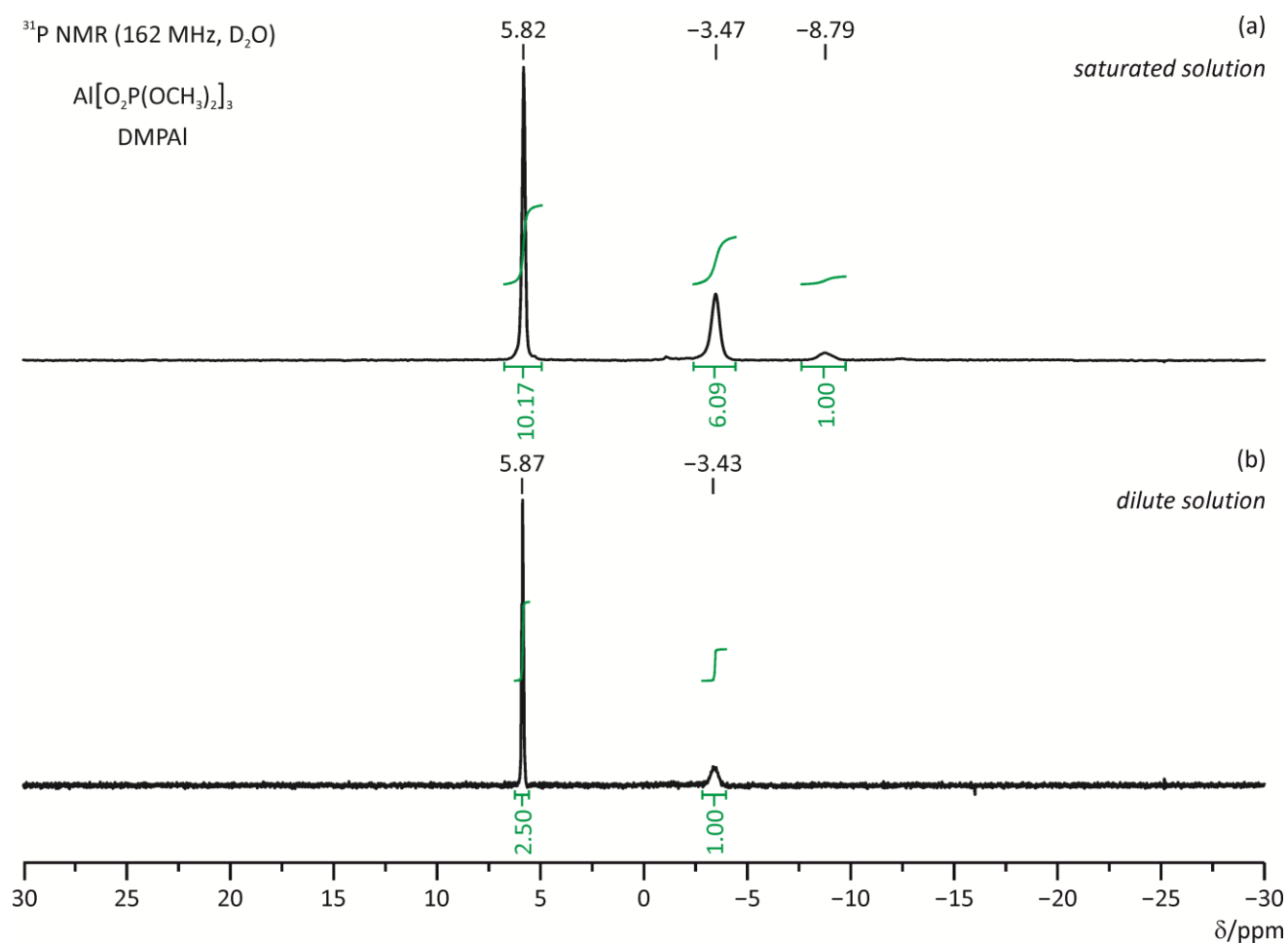


**Figure S13.** <sup>31</sup>P NMR spectra of DMPAI dissolved in D<sub>2</sub>O: saturated solution (a) and dilute solution (b). The spectra were recorded at ambient temperature. The chemical shifts are reported relative to 85% H<sub>3</sub>PO<sub>4</sub> external standard.

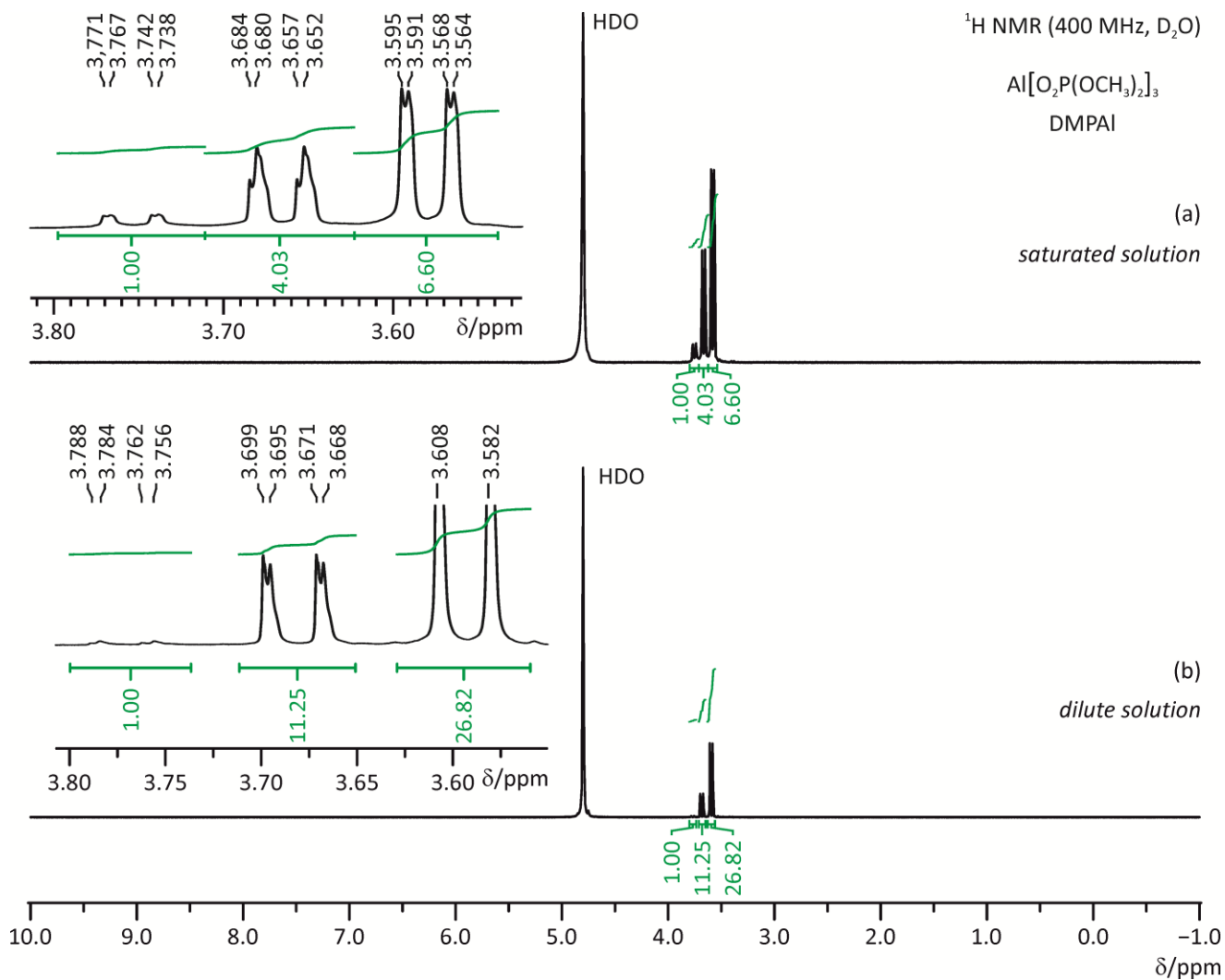


**Figure S14.** <sup>1</sup>H NMR spectra of DMPAI dissolved in D<sub>2</sub>O: saturated solution (a) and dilute solution (b). The spectra were recorded at ambient temperature. The chemical shifts are reported relative to TMS external standard.

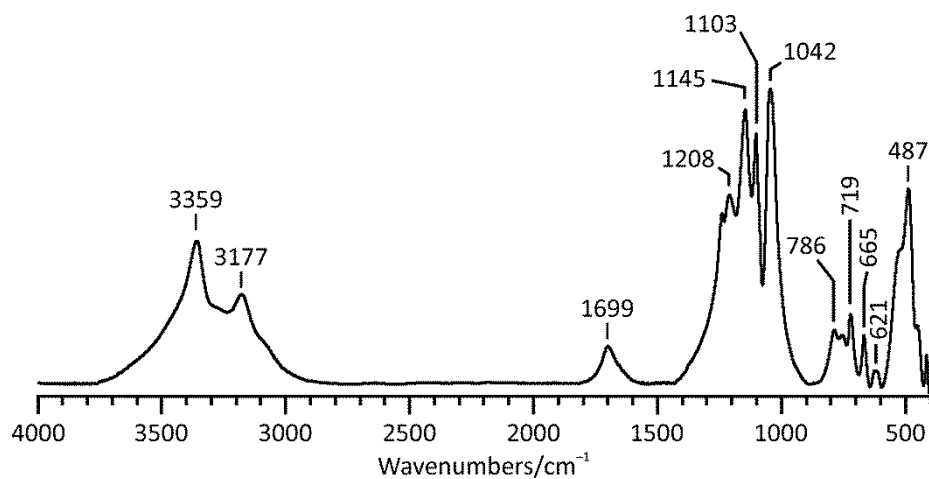
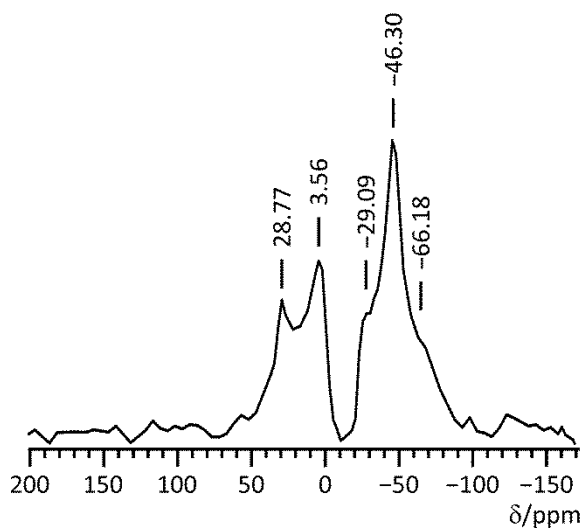


**Figure S15.** FTIR spectrum of a solid product precipitated from a DMPAI aqueous solution heated to 150 °C for 1 h.

(a)  $^{27}\text{Al}$  MAS-NMR [78 MHz]



(b)  $^{31}\text{P}$  MAS-NMR [121 MHz]

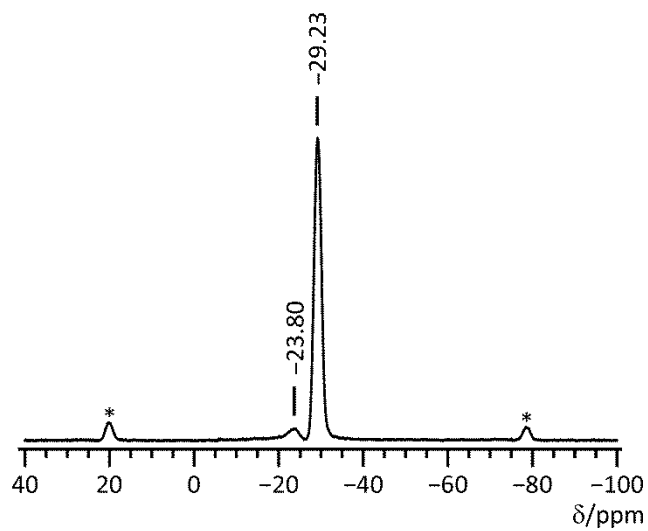


**Figure S16.** MAS NMR spectra of a solid product precipitated from a DMPAl aqueous solution heated to 150 °C for 1 h:  $^{27}\text{Al}$  (a) or  $^{31}\text{P}$  (b). The spectra were recorded at ambient temperature. The asterisks indicate spinning sidebands.